

The statistical description of a chain of interacting Taylor vortices in the direct interaction approximation

V. S. L'vov

Novosibirsk State University

(Submitted 17 September 1980)

Zh. Eksp. Teor. Fiz. 80, 1969-1980 (May 1981)

We show that the traditional method for statistically describing advanced hydrodynamic turbulence by Wyld's diagram technique may turn out to be effective also for the problem of the onset of turbulence when the number of effectively excited degrees of freedom at intermediate Reynolds numbers is still small (say, less than five), while the motion of the liquid is already randomized. We evaluate for noncoinciding times the second moments of the distribution function, which describes the statistics of azimuthal (flexural) modes, for a chain of interacting Taylor vortices that occur after Couette flow with a rotating internal cylinder has lost its stability. The employed direct-interaction approximation which neglects vertex renormalization has enabled us to obtain good qualitative agreement with the results of a numerical experiment [V.S.L.'vov, A. A. Predtechenskii, and A. I. Chernykh, Sov. Phys. JETP 53, No.3 (1981)].

PACS numbers: 47.25.Cg

The problem of the onset of hydrodynamical turbulence has recently been widely discussed. Initially it was assumed that the cause of the random, chaotic motion of the liquid consisted in the excitation of a very large number of degrees of freedom.¹ Subsequently it became clear that simple dynamical systems with phase-space dimensionality larger than two can have a very complex behavior.^{2,3} This is connected with the formation in the phase space of these systems of a stochastic attractor—an attractive set of trajectories which, however, exponentially disperse so that taken separately a trajectory is constrained to become extremely entangled and, in the strict sense, chaotically.

A large number of papers has been devoted to a mathematical analysis of the occurrence of stochasticity of dynamical systems—see, e.g., the survey in Ref. 4 and the literature cited there. Various detailed properties of the Lorenz model are widely discussed in the physical and mathematical literature^{2,5}—this is a set of three ordinary differential equations which are related to the problem of thermal convection in a plane layer.

However, for empirically inclined investigators and experimenters it is important to know not so much the detailed properties of the structure of the attractor—the position of the singular points, the separatrix, and so on—but rather the rough, averaged characteristics of the stochastic behavior of the system: the average size and orientation of the attractor (single-time correlation matrix), frequency the distribution of the energy of the motion (power spectrum), and so on, i.e., quantities which can directly be compared with experiments. For this it is necessary to change from a dynamical description in terms of amplitudes to a statistical description in terms of moments of the distribution function. It is then desirable not to use the detailed information about the actual properties of the attractor, but to refer to it as a black box. One can start from the equations of motion for the amplitudes and obtain in the usual way a chain of equations for the moments and afterwards, hoping that the statistics of the trajectories turns out to be sufficiently simple, close it by decoupling the higher moments in terms of the lower ones, or

perform a partial summation using a diagram technique. This method is used in the theory of turbulence and one usually assumes that it can turn out to be successful for systems with a very large number of degrees of freedom. We show in the present paper that it can be used successfully also in the problem of the onset of hydrodynamic turbulence when, at intermediate Reynolds numbers, the number of effectively excited degrees of freedom is still small while the motion of the liquid is already randomized. To be precise, we consider the following dynamical system:

$$\begin{aligned} dA_n/dt = \gamma A_n + (iT - \eta) |A_n|^2 A_n \\ + i(a + ib)(A_{n+1} + A_{n-1} - 2A_n), \end{aligned} \quad (1)$$

suggested in Ref. 6 to describe the transition to turbulence in Couette-Taylor flow with a rotating internal cylinder. For some $Re = Re_c$, Couette flow in which parts of the liquid move along circles loses its stability and Taylor vortices are formed in which parts of the liquid move along the surfaces of tori. Taylor vortices rotating in different directions are combined into pairs, the interaction between which is shown experimentally to be small compared to the interaction of the vortices which belong to one pair. With increasing Re (when $Re = Re_1$) this flow also loses its stability and the boundary between the vortices in each pair is bent; the quantities $A_n(t)$ are the amplitudes of the bending of the boundary in the pair of number n . The first line in (1) is the usual Landau equation for the amplitude of the secondary flow¹ and the second line describes in the linear approximation the relatively weaker interaction between pairs. It is clear that near the critical Reynolds number Re_1 we can neglect in (1) the dependence of the phenomenological coefficients T , η , a , and b on Re . The coefficient $\gamma = 0$ when $Re = Re_1$ and, hence,

$$\gamma = \alpha(Re - Re_1). \quad (2)$$

The number of equations in (1) is determined by the height of the cylinders. In the experiment in Ref. 6 the number of pairs $N = 15$. Clearly, the equations for the outermost pairs with $n = 1$ and N differ from (1), as they have one rather than two nearest neighbors. Formally, this can be taken into account using the following "bound-

dary conditions”:

$$A_0 = A_{N+1} = 0. \quad (3)$$

It is convenient to change from the variables A_n to the “harmonics representation” which takes the boundary conditions (3) automatically into account and which diagonalizes the linear part of Eqs. (1):

$$B_n = \frac{1}{2(N+1)^{1/2}} \sum_{m=1}^N A_m \sin \frac{\pi mn}{N+1}. \quad (4)$$

We shall expound in §1 Wyld’s diagram technique for Eqs. (1) to (4), taking into account the fact that the harmonics representation (4) differs somewhat from the plane-wave representation. We shall formulate in §2 the equations for the second moment, neglecting vertex renormalization. Usually in the theory of hydrodynamical turbulence one calls this approximation the “direct interaction approximation”—DIA. The DIA equations for our problem are a complicated nonlinear set of $2N$ integral equations. Their detailed analysis—analytical and using a computer—is still to be given. In this paper we take only the first steps in that direction: we obtain in §3 the equations for the energy balance between unstable laminar flows and the system of interacting flexural oscillations; we show in §4 that in the limit as $N \rightarrow \infty$, $\gamma \ll a$ we can find the γ -dependence of the solution of the DIA equations in general form, i. e., we find how it depends on the Reynolds number. In fact

$$I_n(\omega) = \frac{\pi}{16\eta} \left(\frac{a}{2\gamma} \right) f(\kappa, \Omega), \quad (5)$$

where the form of the function f is determined solely by the ratios T/η and b/a while the dimensionless variables κ^2 and Ω are inversely proportional to γ :

$$\kappa^2 = \pi^2 n^2 a / (N+1)^2 \gamma, \quad \Omega = \omega / \gamma. \quad (6)$$

We obtain in §5 an approximate solution of the equations for the structure function f : we show, in particular, that for large κ and Ω the function f decreases exponentially:

$$f(\kappa, \Omega) \propto \kappa \exp[-|\kappa|/\delta - |\Omega|/\Delta],$$

which completely agrees with the results of the numerical experiment performed in Ref. 6 with Eqs. (1) to (3). In the last section, §6, we give a qualitative comparison of the results of the theory developed here with this experiment; we show that the “experimental” and “theoretical” values of the total intensity of the harmonics and also of the effective widths of the distribution in n and in ω differ by not more than 50% (see Table I). In the numerical experiment more than 90% of the energy of motion was concentrated in 3 to 5 harmonics and hence the direct interaction approximation turned out to be successful in a situation where the number of effectively excited degrees of freedom can be counted on the fingers of one hand.

Simpler methods—the self-consistent field approximation or a kinetic equation for the harmonics—simply did not enable us to evaluate the quantity in which we were interested—the distribution $I_n(\omega)$ in ω , i. e., the different-time intensity correlator.

TABLE I. Comparison of the results of a numerical experiment with the conclusion of the theory in the direct interaction approximation.

	$\Gamma = \gamma/a$				Theory
	0.08	0.15	0.2	0.4	$\Gamma \ll 1$
f	0.31	0.31	0.32	0.37	0.38
s_n	0.076	0.12	0.15	0.27	—
p_n	0.086	0.14	0.19	0.38	—
$(s_n/\Gamma)^{1/2}$	0.98	0.90	0.87	0.82	0.66
Δ_+/a	0.051	0.079	0.11	—	—
Δ_-/a	0.045	0.063	0.079	—	—
$(\Delta_+ + \Delta_-)/2\gamma$	0.60	0.48	0.47	—	0.84

§1. DIAGRAM TECHNIQUE

In the harmonics representation (4), Eqs. (1) take the form

$$dB_n/dt = -(\gamma_n + ib_n)B_n + (NL)_n, \quad (1.1)$$

where

$$\gamma_n = (-\gamma + a_n), \quad a_n = a \sin^2 \frac{\pi n}{2(N+1)}, \quad (1.2)$$

$$b_n = b \sin^2 [\pi n/2(N+1)].$$

The nonlinear part of (1.1) is rather complicated in form:

$$(NL)_n = \frac{iD}{2} \sum_{n_1, n_2, n_3 = -N}^N B_1 B_2 B_3 [\Delta(n+n_1+n_2+n_3) + \Delta(n+n_1+n_2+n_3+2N+2) + \Delta(n+n_1+n_2+n_3-2N-2)], \quad (1.3)$$

$$D = 8(T + i\eta)/(N+1).$$

Here $B_i = B_n$, $B_{-n} = -B_n$, and Δ is the Kronecker symbol: $\Delta(0) = 1$, $\Delta(n) = 0$, when $n \neq 0$.

Following Wyld’s idea⁷ we include in the right-hand side of the initial equations of motion (1.1) the random force $f_n(t)$ which imitates the jolts from the “surrounding medium.” We shall assume that $f_n(t) = -f_{-n}(t)$ and that its statistical properties are Gaussian with correlators

$$\langle f_n(t) f_m^*(t') \rangle = \delta(t-t') [\Delta(m-n) - \Delta(m+n)] f_n^2. \quad (1.4)$$

In the ω -representation Eqs. (1.1) and (1.2) take the form

$$B_n(\omega) = G_n^0(\omega) \left\{ \frac{D}{2} \sum_{i=1,2,3} \int \delta(\omega + \omega_i - \omega_2 - \omega_3) \right. \quad (1.5)$$

$$\times [\Delta(n+n_1+n_2+n_3) + \Delta(n_1+n_2+n_3+2N+2) + \Delta(n+n_1+n_2+n_3-2N-2)] B_1 B_2 B_3 d\omega_1 d\omega_2 d\omega_3,$$

where $B_i = B_{n_i}(\omega_i)$, $i = 1, 2, 3$, G_n^0 is the bare Green function:

$$G_n^0 = [\omega + b_n - i\gamma_n]^{-1}, \quad (1.6)$$

in which b_n and γ_n are given by Eqs. (1.2). Iterating these equations we can write $B_n(\omega)$ as a power series in $f_n(\omega)$.

We now determine the Green function $G_n(\omega)$:

$$\left\langle \frac{\delta B_n(\omega)}{\delta f_m(\omega')} \right\rangle = G_n(\omega) \delta(\omega - \omega') [\Delta(n-m) - \Delta(n+m)] \quad (1.7)$$

and introduce the graph notation:

$$e_n(\omega) = \longrightarrow, \quad e_n^*(\omega) = \longleftarrow.$$

We define the pair correlator $I_n(\omega)$ as

$$\langle B_n(\omega) B_m^*(\omega') \rangle = I_n(\omega) \delta(\omega - \omega') [\Delta(n-m) - \Delta(n+m)] \quad (1.8)$$

and put

$$I_h(\omega) = \text{~~~~~}, \quad I_h^*(\omega) = \text{~~~~~}.$$

We have assumed here that the correlation matrix $\langle B_n(t) B_m^*(t') \rangle$ is diagonal in n, m . This assumption is exact in the limit as $N \rightarrow \infty$ when translational symmetry arises in the system. In the numerical experiment of Ref. 6 (the procedure of which is briefly described in §6) the coefficient of correlations between even and odd harmonics $K_{n,2m}$ is less than 10^{-2} . Here

$$K_{mn} = |\langle B_m B_n^* \rangle| / [|\langle B_m \rangle|^2 |\langle B_n \rangle|^2].$$

Odd harmonics turned out to be most strongly correlated, but this correlation decreases rapidly with increasing γ . For instance, when $b/a = 1.25$ and $T/\eta = 10$, $K_{1,3} = 0.31; 0.11; 0.014; 0.006$, respectively for $\gamma/a = 0.08; 0.15; 0.2; 0.4$.

By summing in the usual way⁸ the weakly coupled diagrams we can arrive at a set of Dyson equations for G_n and I_n :

$$\begin{aligned} G_n^{-1}(\omega) &= \omega + b_n - i\gamma_n - \Sigma_n(\omega), \\ I_n(\omega) &= |G_n|^2 \Phi_n(\omega). \end{aligned} \quad (1.9)$$

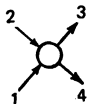
Here Σ_n and Φ_n are the sums of compact diagrams. In Σ_n we can pass from the ingoing to the outgoing point along G lines; Φ_n can be uniquely cut along the I lines.

We give the first diagrams:

$$\Sigma_n = \text{~~~~~} + \text{~~~~~} + \frac{1}{2} \text{~~~~~} + \dots \quad (1.10)$$

$$\Phi_n = \frac{1}{2} \text{~~~~~} + \text{~~~~~} + \dots \quad (1.11)$$

In these we must assign to each line its number n and index ω , and associate with each open vertex



the expression

$$\begin{aligned} & D \sum_{\sigma_1, \sigma_2, \sigma_3, \sigma_4 = \pm 1} \delta(\omega_1 + \omega_2 - \omega_3 - \omega_4) \\ & \times \left[\Delta \left(\sum_{i=1}^4 \sigma_i n_i \right) + \Delta \left(\sum_{i=1}^4 \sigma_i n_i + 2N + 2 \right) + \Delta \left(\sum_{i=1}^4 \sigma_i n_i - 2N - 2 \right) \right]. \end{aligned}$$

The filled vertices are the complex conjugates of the open ones. We must sum over all internal numbers n from 1 to $N+1$ and integrate from $-\infty$ to ∞ over all internal frequencies.

§2. DIRECT INTERACTION APPROXIMATION

If in the series (1.10) for Σ_n we retain only the first diagram and put $\Phi_n = 0$, we get for $I_n(\omega)$ a simple set of equations

$$\left\{ -i\omega - (\gamma + ib_n) + iD \int \left[\sum_{m=-N}^N I_m(\omega') + I_n(\omega) \right] d\omega' \right\} I_n(\omega) = 0, \quad (2.1)$$

or, in the τ -representation

$$\frac{dI_n(\tau)}{d\tau} = I_n(\tau) \left\{ -(\gamma_n + ib_n) + iD \left[\sum_{m=-N}^N I_m(0) + I_n(0) \right] \right\}. \quad (2.2)$$

We can obtain these equations directly from (1.1) and (1.2) if we decouple the fourth moment in terms of products of binary ones. It is clear from (2.1) and (2.2) that this approximation is equivalent to the self-consistent field approximation when in the equation of motion for $I_n(\tau)$ all remaining harmonics are replaced by their time-averaged values. Of course, this approximation is very far from reality, but all the same it shows up one tendency correctly: the region (in the numbers n) of the effectively excited harmonics may turn out to be narrower than the region in which the linear growth rate is positive (i.e., $\gamma > a_n$). In particular, there follows from (2.2) an expression for the threshold for the excitation of the second harmonic:

$$\gamma - a_2 = 2(a_2 - a_1) > 0. \quad (2.3)$$

We obtain a much more realistic approximation if we take into account in the series (1.10) and (1.11) for Σ_n and Φ_n also the diagrams with two vertexes. Then

$$\begin{aligned} \Sigma_n(\omega) &= D \int \left[\sum_{i=-N}^N I_i + I_n(\omega_i) \right] d\omega_i \\ &+ \frac{1}{2} \int \delta(\omega + \omega_1 - \omega_2 - \omega_3) \sum_{i_1, i_2, i_3 = -N}^N \Delta(n + n_1 + n_2 + n_3) \\ &\quad \times [1 + \Delta(n + n_1) + \Delta(n + n_2) + \Delta(n + n_3)] \\ &\quad \times [|D|^2 G_1 G_2 I_3 + D^2 I_1 (I_2 G_3 + G_2 I_3)] d\omega_1 d\omega_2 d\omega_3, \\ \Phi_n(\omega) &= \frac{|D|^2}{2} \int \delta(\omega + \omega_1 - \omega_2 - \omega_3) \sum_{i_1, i_2, i_3 = -N}^N \Delta(n + n_1 + n_2 + n_3) \\ &\quad \times [1 + \Delta(n + n_1) + \Delta(n + n_2) + \Delta(n + n_3)] I_1 I_2 I_3 d\omega_1 d\omega_2 d\omega_3. \end{aligned} \quad (2.4)$$

Kraichnan has made an analogous approximation in the theory of developed hydrodynamic turbulence, starting directly from the Navier-Stokes equations, and he called it the direct interaction approximation—DIA. Such an approximation is somewhat broader than allowance for the interaction in second order in the vertex (i.e., in our case the decoupling of the sixth-order correlators in terms of binary ones). It includes also a self-consistency procedure that leads to the replacement of the initial damping and eigenfrequency of the harmonics ($\gamma_n + ib_n$) by effective quantities ($\gamma_n + ib_n$) + $\Sigma_n(\omega)$ which depend on the characteristics of the motion.

To determine the region of applicability of the DIA it is necessary to obtain the solution of Eqs. (1.9) and (2.4) and to evaluate in them diagrams with three vertices in the series (1.10) and (1.11) for Σ_n and Φ_n , which give the first correction to the DIA. One can assume the DIA to be reasonable far from the bifurcation lines which separate, in the parameter plane, the region of the stochastic attractor from the region with regular behavior-of limit cycles and equilibrium positions. The $M_n(\omega)$ excess graphs given in Figs. 10 and 11 of Ref. 6 and obtained in the numerical experiment

are an argument in favor of this. It is clear that M_n is close to unity, as should be the case for Gaussian statistics of the random processes $B_n(t)$.

§3. ENERGY BALANCE EQUATION

From the set of Dyson equations (1.9) we can obtain the energy balance equation

$$\text{Im} [I_n(\omega)\Sigma_n(\omega) - G_n(\omega)\Phi_n(\omega)] = 0, \quad (3.1)$$

which goes over into the kinetic equation in the limiting case of a weak interaction ($\Sigma_n \ll a_n, b_n$). If we integrate (3.1) over ω and sum over n , the terms with a Hamiltonian structure (proportional to T^2) which describe the exchange of energy between harmonics cancel. The integral equation obtained will describe the energy exchange between laminar Couette-Taylor flow and its perturbation—a system of interacting azimuthal (flexural) oscillations:

$$W_0 = W_1 + W_2. \quad (3.2)$$

Here W_0 is the energy flux from the unstable laminar flow into the oscillations:

$$W_0 = \int \sum_{n=-N}^N I_n(\omega) (\gamma - a_n) d\omega, \quad (3.3)$$

W_1 is the nonlinear energy dissipation due to their reaction on the flux:

$$W_1 = \frac{8\eta}{N+1} \sum_{m,n=-N}^N I_n(\omega) I_m(\omega') [1 + \Delta(m+n)] d\omega d\omega'. \quad (3.4)$$

We can interpret the terms in second order in the interaction W_2 as the distortion of W_1 due to the interaction between oscillations:

$$W_2 = \frac{128\eta}{(N+1)^2} \sum_{i_1, i_2, i_3, i_4} \int I_{i_1} I_{i_2} I_{i_3} I_{i_4} [(T + i\eta) G_i] \times \Delta(n_1 + n_2 + n_3 + n_4) [1 + \Delta(n_1 + n_2) + \Delta(n_1 + n_3) + \Delta(n_1 + n_4)] \delta(\omega_1 + \omega_2 - \omega_3 - \omega_4) d\omega_1 d\omega_2 d\omega_3 d\omega_4. \quad (3.5)$$

In the "direct interaction approximation" used by us the terms of higher order in the interaction W_3, W_4, \dots are neglected. The expression for W_2 can be identically transformed into an essentially simpler form, if we use the second of the Dyson Eqs. (1.9) and the explicit expression for Φ_n :

$$W_2 = \frac{4\eta}{T^2 + \eta^2} \sum_{n=-N}^N \int d\omega I_n(\omega) \text{Im} \left[\frac{iT - \eta}{G_n(\omega)} \right]. \quad (3.6)$$

Substituting here Eq. (1.9) for G_n we get

$$W_2 = \frac{4\eta}{T^2 + \eta^2} \sum_{n=-N}^N \int d\omega I_n(\omega) \text{Im} [(iT - \eta)(\omega + b_n - i\eta - ia_n - \Sigma_n(\omega))]. \quad (3.7)$$

It is clear that in the case of most interest for the experiment, $T \gg \eta$, W_2 is small compared to W_0 by a factor η/T . Hence, when $T \gg \eta$ we may assume that $W_0 = W_1$. The role of the interactions between the harmonics ($\propto T^2$) is then reduced to the widening of the packet I_n in n and decrease in energy input W_0 corresponding to this. In the limit as $\eta/T \rightarrow 0$ in general $W_1 \rightarrow 0$.

§4. SCALING IN THE DIA EQUATIONS

In the experiment of Ref. 6 the number of vortex pairs $N = 15$. To simplify the analysis of the equations we shall assume that $N \rightarrow \infty$ and change from a summation over n to an integration over the dimensionless variable

$$k = n/(N+1). \quad (4.1)$$

Subsequently we show that when $\gamma \ll a$ the packet of excited harmonics is narrow: $k^2 \approx \gamma/a$. The bar means here averaging with weight I_n :

$$\bar{\Psi} = \int \Psi_n I_n dk / \int I_n dk. \quad (4.2)$$

Assuming henceforth that $\gamma \ll a$ we expand a_n and b_n in a series in k , limiting ourselves to the first term and we extend the integration over k over the infinite domain. In the initial equations thus simplified we can eliminate the γ -dependence if we change to the dimensionless variables:

$$I_{k\omega} = f(x, \Omega) / 8\eta k_0, \quad G_{k\omega} = g(x, \Omega) / \gamma, \quad (4.3)$$

$$\Omega = \omega / \gamma, \quad x = k / k_0, \quad k_0^2 = 4\gamma / \pi^2 a. \quad (4.4)$$

In these variables the Dyson Eqs. (1.9) take the form

$$g^{-1}(x, \Omega) = \Omega + Bx^2 + i - ix^2 - \sigma(x, \Omega), \quad (4.5)$$

$$f(x, \Omega) = |g(x, \Omega)|^2 \varphi(x, \Omega),$$

where σ and φ are dimensionless mass operators:

$$\sigma(x, \Omega) = \Sigma_n(\omega) / \gamma, \quad (4.6)$$

$$\varphi(x, \Omega) = 8\eta k_0 \Phi_n(\omega) / \gamma^2$$

and where we have used the notation

$$B = b/a, \quad \Theta = T/\eta. \quad (4.7)$$

From (2.4) it follows for σ and φ that

$$\sigma(x, \Omega) = f + \frac{1}{2}(\Theta^2 + 1)(g^* \times f \times g)_{x, \Omega} + (\Theta + i)^2 (f \times f \times g)_{x, \Omega}, \quad (4.8)$$

$$\varphi(x, \Omega) = \frac{1}{2}(\Theta^2 + 1)(f \times f \times f)_{x, \Omega},$$

where

$$f = \int f(x) dx, \quad f(x) = \int f(x, \Omega) d\Omega \quad (4.9)$$

and where we have introduced for the convolution the notation:

$$(\alpha \times \beta \times \gamma)_{x, \Omega} = \int \alpha(x_1, \Omega_1) \beta(x_2, \Omega_2) \gamma(x_3, \Omega_3) \delta(x + x_1 - x_2 - x_3) \times \delta(\Omega + \Omega_1 - \Omega_2 - \Omega_3) dx_1 dx_2 dx_3 d\Omega_1 d\Omega_2 d\Omega_3. \quad (4.10)$$

The equations (4.5) to (4.9) which we have obtained for the structure functions $f(x, \Omega)$ and $g(x, \Omega)$ no longer contain the coefficient γ which depends on the Reynolds number; the form of these functions can thus depend only on the dimensionless ratios B and Θ [see (4.7)]. Hence, the whole dependence on γ is completely determined by Eqs. (4.3) and (4.4), and this conclusion is not connected with the direct interaction approximation. An important restriction are only the inequalities

$$(N+1)^{-2} \ll \gamma/a \ll 1, \quad (4.11)$$

which lead to the fact that the number of excited harmonics is small compared to their total number N and large compared to unity.

It follows, in particular, from Eqs. (4.3) and (4.4) that the width of the function $I_n(\omega)$ in ω is proportional

to γ , the number of the excited harmonics (the width of I_n in n) proportional to $(\gamma/a)(N+1)$, and the average intensity I of the harmonics is also proportional to γ :

$$I = \frac{1}{N+1} \sum_{n=1}^N \int I_n(\omega) d\omega = \frac{\gamma f_{\text{pe}}}{16\eta}. \quad (4.12)$$

It will be shown in §6 that all these conclusions are confirmed by the numerical experiment.

§5. PRELIMINARY ANALYSIS OF THE STRUCTURE FUNCTIONS

We first simplify the Green function. The first term in (4.8) for $\sigma(\kappa, \Omega)$ is completely independent of Ω . We shall neglect the Ω -dependence also in the second term, putting there $\Omega = \Omega_0$ where Ω_0 is a root of the equation

$$\Omega = \text{Re } \sigma(0, \Omega). \quad (5.1)$$

We shall also neglect the κ -dependence of σ as compared to the quadratic κ -dependence of the bare quantities a_n and b_n . The Green function $g(\kappa, \Omega)$ then takes on a simple form

$$g^{-1} = (\Omega + B\kappa^2) - i(\bar{\gamma} + \kappa^2). \quad (5.2)$$

Here Ω is reckoned from the line center Ω_0 and the role of the interaction is reduced to the renormalized damping:

$$\bar{\gamma} = -1 + \text{Im } \sigma(0, \Omega_0). \quad (5.3)$$

We shall see below that this approximation for the Green function enables us to obtain qualitatively correct results. Using this we appreciably simplify Eq. (4.5) for the structure function of the pair correlator:

$$f(\kappa, \Omega) = \frac{(\theta^2 + 1)(f \times f \times f)_{\kappa, \Omega}}{2[(\Omega + B\kappa^2)^2 + (\bar{\gamma} + \kappa^2)^2]}, \quad (5.4)$$

where the convolution $(f \times f \times f)$ is determined by Eq. (4.10).

In these equations the Green function $g(\kappa, \Omega)$ is determined by the sole constant $\bar{\gamma}$. We can therefore use instead of the Dyson equation for $g(\kappa, \Omega)$ the appreciably simpler energy balance Eq. (3.2) to (3.7). In dimensionless variables it has the form

$$1 + \bar{\kappa}^2 + f + \frac{4\theta(\bar{\Omega} + B\bar{\kappa}^2 + \bar{\kappa}^2 + \bar{\gamma})}{\theta^2 + 1}, \quad (5.5)$$

where the bar indicates averaging with weight $f(\kappa, \Omega)$:

$$\bar{\Psi} = \int \Psi(\kappa, \Omega) f(\kappa, \Omega) d\kappa d\Omega / f. \quad (5.6)$$

Equations (5.4) and (5.5) for the function $f(\kappa, \Omega)$ and the constant $\bar{\gamma}$ are closed. We have not been able to obtain their analytical solution. We can indicate only the asymptotic behavior of $f(\kappa, \Omega)$ for large κ, Ω :

$$f(\kappa, \Omega) \propto \kappa \exp(-|\kappa|/\delta - |\Omega|/\Delta), \quad (5.7)$$

where the constants δ and Δ are of order unity. To determine them we must obtain a solution of Eq. (5.4) for the whole range of κ and Ω . For this we use the method of successive approximations. First of all we try to guess a sufficiently wide zeroth approximation function $f_0(\kappa, \Omega)$ and then, substituting it into the right-hand side of (5.4) we get an answer for $f(\kappa, \Omega)$ in first approximation; we determine the constants δ and Δ from the con-

dition that the function $f_0(\kappa, \Omega)$ be as close as possible to $f_1(\kappa, \Omega)$ in that range of κ and Ω where these functions are sufficiently large.

For $f_0(\kappa, \Omega)$ we take the expression

$$f_0(\kappa, \Omega) = f_0 \frac{2\kappa}{\pi^2 \delta^2 \Delta} \left(\text{sh } \frac{\kappa}{\delta} \text{ch } \frac{\Omega}{\Delta} \right)^{-1}, \quad (5.8)$$

which has an obvious maximum when $\kappa = \Omega = 0$, has the asymptotic form (5.7) for large κ, Ω , and is chosen such that the convolution in the right-hand side of (5.4) can be evaluated analytically. We then get for $f_1(\kappa, \Omega)$ the following expression:

$$f_1(\kappa, \Omega) = f_0(\kappa, \Omega) \frac{(\theta^2 + 1) f_0^2 (\Omega^2 + \Omega_0^2) (\kappa^2 + 2\kappa_0^2) (\kappa^2 + 8\kappa_0^2)}{30\Omega_0^2 \kappa_0^4 [(\Omega + B\kappa^2)^2 + (\bar{\gamma} + \kappa^2)^2]}. \quad (5.9)$$

Here

$$\Omega_0^2 = (\pi\Delta)^2/4, \quad \kappa_0^2 = \pi\delta^2/2. \quad (5.10)$$

We note that the Ω -dependence of $f(\kappa, \Omega)$ is apparently determined by the interaction between the strongest harmonics with $\kappa \lesssim \kappa_0$. These harmonics serve as a forcing force for the far harmonics and they impose on them their frequency spectrum. For its analysis it is thus natural to make the zeroth and first approximation agree as $\kappa \rightarrow 0$. The condition $f_1(0, \Omega) = f_0(0, \Omega)$ gives

$$\Omega_0 = \bar{\gamma} = [2(\theta^2 + 1)/15]^{1/2} f_0. \quad (5.11)$$

We can obtain one more relation by using the integral relation following from (5.4):

$$\bar{\Omega}^2 + 2B\bar{\Omega}\bar{\kappa}^2 + B^2\bar{\kappa}^4 + \bar{\gamma}^2 + 2\bar{\gamma}\bar{\kappa}^2 + \bar{\kappa}^4 = (\theta^2 + 1)f^2/2. \quad (5.12)$$

Performing the averaging with the function $f_0(\kappa, \Omega)$ we get

$$\Omega_0^2 + \bar{\gamma}^2 + 2\bar{\gamma}\kappa_0^2 + 4(B^2 + 1)\kappa_0^4 = (\theta^2 + 1)f_0^2/2. \quad (5.13)$$

These relations are closed by the balance Eq. (5.5):

$$1 = \kappa_0^2 + f + \frac{(4\theta B + 1)\kappa_0^2 + \bar{\gamma}}{\theta^2 + 1}. \quad (5.14)$$

Assuming $\theta^2 \gg 1$ for the sake of simplicity we write down the solution of Eqs. (5.12) and (5.13):

$$\bar{\gamma} = \Omega_0 = 4(B^2 + 1)\kappa_0^2 / [(7B^2 + 8)^{1/2} - 1] = \theta f (2/15)^{1/2},$$

$$f_0 = \frac{2\sqrt{30}(B^2 + 1)}{2\sqrt{30}(B^2 + 1) + (\theta + 4B)[(7B^2 + 8)^{1/2} - 1]}. \quad (5.15)$$

In what follows we compare these expressions with the results of a numerical modeling.⁶

§6. COMPARISON WITH THE RESULTS OF A NUMERICAL EXPERIMENT

In Ref. 6 the set of Eqs. (1) to (3) was solved by a computer; as a result we found the trajectories of $A_n(t)$ at times much larger than the characteristic periods of the motion. We chose the number N of the equations in accordance with the experiment of Ref. 6: $N = 15$. We showed that depending on the parameters of the equations B, θ , and $\Gamma = \gamma/a$ the trajectories of $A_n(t)$ can move to a stable point, or a limit cycle, or demonstrate a complicated behavior which from the point of view of an experimenter is stochastic.

We evaluated the spectra $I_n(\omega)$ for $\Theta = 10$, $B = 1.25$, and four values of $\Gamma = 0.08$; 0.15 ; 0.2 ; 0.4 which fall in the region of stochastic behavior—see Fig. 7 of Ref. 6. We note first of all that both the theory and the numerical experiment give an exponential decrease of $I_n(\omega)$ far from the line center. It is true that the arguments of the exponential Δ_n in the numerical experiment was different for the right- and the left-hand slopes of the curve, while the line shape (5.8) in the zeroth approximation is symmetric. A certain asymmetry in the line appears only in the first approximation—see (5.11).

The exponential decrease of I_n with increasing n predicted by Eq. (5.8) is also well satisfied in the numerical experiment—see Tables II and IV of Ref. 6. The difference in the behavior of the even and the odd harmonics observed in the numerical experiment disappeared from the theory in the limit as $N \rightarrow \infty$.

In Table I we give the results of the numerical experiment for the total intensity of the harmonics $I = \sum_n I_n$, of the quantities

$$s_n = \overline{\sin^2 \frac{\pi n}{32}}, \quad p_n = \overline{\left(\frac{\pi n}{32} \right)^2},$$

which characterize the width of the packet I_n in n :

$$\overline{n^2} = \sum_n n^2 I_n / \sum_n I_n$$

and the indexes Δ_n determining the asymptotic behavior of $I_n(\omega)$ with respect to the frequencies. In correspondence with the theory, the quantities $f = \eta l / \gamma$, n^2 / γ and Δ / γ should be independent of γ in the region above the critical point, satisfying the inequalities (4.11). Indeed, when we change Γ by a factor 5 these quantities change by less than 25%. This small change is

caused by the violation of the inequality $\Gamma \ll 1$, which enabled us to restrict ourselves in the expansion of $\sin(\pi n / 32)$ to the first term. It is clear from Table I that the quantities s_n are noticeably smaller than p_n and that this difference increases with increasing Γ .

On the right-hand side of Table I we give the values of the corresponding quantities calculated by using the approximate Eqs. (5.15) and (5.10). They differ from the experimental ones by not more than 50%. It is just now difficult to say whether this difference is connected with the direct interaction approximation itself which is used in deriving Eqs. (1.9) and (2.4) or with the assumptions made when analyzing these equations.

¹L. D. Landau, Dokl. Akad. Nauk SSSR 44, 339 (1944) [Collected Papers of L. D. Landau, Pergamon Press, Oxford, 1965, p. 387].

²E. Lorenz, J. Atmos. Sc. 20, 130 (1963).

³M. I. Rabinovich, Usp. Fiz. Nauk 125, 123 (1978) [Sov. Phys. Usp. 21, 443 (1978)].

⁴Ya. G. Sinaĭ, Stokhastichnost' dinamicheskikh sistem (Stochasticity of dynamical systems) in Nelineĭnye volny (Non-linear waves) Ed. A. V. Gaponova-Grekhova, Nauka, Moscow, 1979.

⁵L. A. Bunimovich and Yu. G. Sinaĭ, Stokhastichnost' attraktora v modeli Lorentsa (Stochasticity of the attractor in the Lorenz model) in Nelineĭnye volny (Non-linear waves) Ed. A. V. Gaponova-Grekhova, Nauka, Moscow, 1979.

⁶V. S. L'vov, A. A. Predtechenskiĭ, and A. I. Chernykh, Zh. Eksp. Teor. Fiz. 80, 1099 (1981) [Sov. Phys. JETP 53, (1981)].

⁷H. Wyld, Ann. Phys. 14, 143 (1961).

⁸V. E. Zakharov and V. S. L'vov, Izv. Vyssh. Uchebn. Zaved. Radiofiz. 18, 1470 (1975) [Radiophys. Qu. Electron. 18, 1084 (1976)].

Translated by D. ter Haar